REPORT DOCUMENTATION PAGE

Form Approved OMB NO. 0704-0188

1. REPORT DATE (DD-MM-YYYY)	2. REPORT TYPE	3. DATES COVERED (From - To)
05-05-2011	Final Report	10-Aug-2010 - 9-Apr-2011

4. TITLE AND SUBTITLE
Development and Application of a Soil Moisture Downscaling Method for Mobility Assessment

5a. CONTRACT NUMBER
W911NF-10-1-0373

5b. GRANT NUMBER

5c. PROGRAM ELEMENT NUMBER
622784

6. AUTHORS
M.L. Coleman, J.D. Niemann

5d. PROJECT NUMBER

5e. TASK NUMBER

5f. WORK UNIT NUMBER

7. PERFORMING ORGANIZATION NAMES AND ADDRESSES
Colorado State University - Ft. Collins
Office of Sponsored Programs
Colorado State University
Fort Collins, CO 80523 -2002

8. PERFORMING ORGANIZATION REPORT NUMBER

9. SPONSORING/MONITORING AGENCY NAME(S) AND ADDRESS(ES)
U.S. Army Research Office
P.O. Box 12211
Research Triangle Park, NC 27709-2211

10. SPONSOR/MONITOR'S ACRONYM(S)
ARO

11. SPONSOR/MONITOR'S REPORT NUMBER(S)
57411-EV-II.1

12. DISTRIBUTION AVAILIBILITY STATEMENT
Approved for Public Release; Distribution Unlimited

13. SUPPLEMENTARY NOTES
The views, opinions and/or findings contained in this report are those of the author(s) and should not contrued as an official Department of the Army position, policy or decision, unless so designated by other documentation.

14. ABSTRACT
Soil moisture is a critical variable for many Army activities including mobility assessments. Several methods can be used to produce soil moisture patterns at an intermediate resolution (grid cells with ~1 km linear dimension). However, mobility assessments require fine-resolution estimates (~30 m grid cells). Thus, a method is required to downscale intermediate-resolution patterns to finer resolutions. Fortunately, fine-resolution variations in soil moisture are known to depend on various topographic attributes, and topographic data are available at

15. SUBJECT TERMS
Soil, moisture, downscaling, disaggregation, topography, wetness

16. SECURITY CLASSIFICATION OF:			17. LIMITATION OF ABSTRACT	15. NUMBER OF PAGES	19a. NAME OF RESPONSIBLE PERSON
a. REPORT	b. ABSTRACT	c. THIS PAGE			Jeffrey Niemann
UU	UU	UU	UU		19b. TELEPHONE NUMBER: 970-491-3517

Report Title

Development and Application of a Soil Moisture Downscaling Method for Mobility Assessment

ABSTRACT

Soil moisture is a critical variable for many Army activities including mobility assessments. Several methods can be used to produce soil moisture patterns at an intermediate resolution (grid cells with ~1 km linear dimension). However, mobility assessments require fine-resolution estimates (~30 m grid cells). Thus, a method is required to downscale intermediate-resolution patterns to finer resolutions. Fortunately, fine-resolution variations in soil moisture are known to depend on various topographic attributes, and topographic data are available at fine-resolutions for almost any region on Earth. The overall objective of this project is to develop, calibrate, and apply a method to estimate fine-scale soil moisture patterns based on intermediate-resolution soil moisture estimates and the observed topographic dependence of soil moisture. The method is a conceptual model that estimates soil moisture values by assuming that the soil moisture pattern is at equilibrium and by inferring the spatial variations of vadose-zone processes from topographic characteristics. The method is calibrated using the Tarrawarra and Cache la Poudre catchments, which have extensive soil moisture datasets. It is then applied to a region of interest in Afghanistan for dry, wet, and very wet scenarios where only intermediate-resolution estimates are available.

List of papers submitted or published that acknowledge ARO support during this reporting period. List the papers, including journal references, in the following categories:

(a) Papers published in peer-reviewed journals (N/A for none)

Number of Papers published in peer-reviewed journals: 0.00

(b) Papers published in non-peer-reviewed journals or in conference proceedings (N/A for none)

Number of Papers published in non peer-reviewed journals: 0.00

(c) Presentations

Coleman, M.L, and J.D. Niemann, March 2011, "A Conceptual Model for Soil Moisture Estimation and Downscaling Based on Topographic Attributes," American Geophysical Union Hydrology Days, Fort Collins, Colorado.

Kampf, S., and J.D. Niemann, March 2011, "Basin and catchment-scale hydrologic regimes in the Cache la Poudre," Interdisciplinary Water Resources Seminar, Colorado State University, Fort Collins, Colorado.

Niemann, J.D., F.A. Busch, and M.L. Coleman, March 2011, "Evaluation of a Method to Estimate Ponded Locations for Use in MyWida/T-IWEDA," Oral Presentation, DoD Center for Geosciences/Atmospheric Research, Colorado State University, Fort Collins, Colorado.

Busch, F.A., J.D. Niemann, M.L. Coleman, and C.M. Fields, March 2011, "Evaluation of a Method to Estimate Ponded Locations for Use in MyWida/T-IWEDA," Poster Presentation, DoD Center for Geosciences/Atmospheric Research, Colorado State University, Fort Collins, Colorado.

Niemann, J.D., F.A. Busch, M.L. Coleman, and B.M. Lehman, August 2010, "Evaluating Methods to Downscale Soil Moisture Based on Topography," Engineering Research and Development Center, Vicksburg, Mississippi.

Niemann, F.A. Busch, M.L. Coleman, and B.M. Lehman, August 2010, "Downscaling Soil Moisture based on Topography: A Ponding Algorithm for T-IWEDA," Interagency Land Surface Dynamics Coordination Meeting, Engineering Research and Development Center, Vicksburg, Mississippi.

Number of Presentations: 6.00

Non Peer-Reviewed Conference Proceeding publications (other than abstracts):

Number of Non Peer-Reviewed Conference Proceeding publications (other than abstracts): 0

Peer-Reviewed Conference Proceeding publications (other than abstracts):

Number of Peer-Reviewed Conference Proceeding publications (other than abstracts): 0

(d) Manuscripts

Busch, F.A., J.D. Niemann, and M.L. Coleman, 2011, "Evaluation of the Portability of an EOF-Based Method to Downscale Soil Moisture Patterns Based on Topographical Attributes," Hydrologic Processes, in review.

Coleman, M.L., and J.D. Niemann, 2011, "An evaluation of nonlinear methods for estimating catchment-scale soil moisture patterns based on topographic attributes," Journal of Hydroinformatics, in review.

Number of Manuscripts: 2.00

Patents Submitted

Patents Awarded

Awards

Niemann, J.D., Borland Chair of Hydrology, Department of Civil and Environmental Engineering, Colorado State University (2010)

Graduate Students

NAME	PERCENT_SUPPORTED
Michael Coleman	1.00
Andre Dozier	0.25
FTE Equivalent:	**1.25**
Total Number:	**2**

Names of Post Doctorates

NAME	PERCENT_SUPPORTED
FTE Equivalent:	
Total Number:	

Names of Faculty Supported

NAME	PERCENT_SUPPORTED	National Academy Member
Jeffrey D. Niemann	0.06	No
FTE Equivalent:	**0.06**	
Total Number:	**1**	

Names of Under Graduate students supported

NAME	PERCENT SUPPORTED

FTE Equivalent:

Total Number:

Student Metrics

This section only applies to graduating undergraduates supported by this agreement in this reporting period

The number of undergraduates funded by this agreement who graduated during this period:	0.00
The number of undergraduates funded by this agreement who graduated during this period with a degree in science, mathematics, engineering, or technology fields:.....	0.00
The number of undergraduates funded by your agreement who graduated during this period and will continue to pursue a graduate or Ph.D. degree in science, mathematics, engineering, or technology fields:.....	0.00
Number of graduating undergraduates who achieved a 3.5 GPA to 4.0 (4.0 max scale):	0.00
Number of graduating undergraduates funded by a DoD funded Center of Excellence grant for Education, Research and Engineering:	0.00
The number of undergraduates funded by your agreement who graduated during this period and intend to work for the Department of Defense	0.00
The number of undergraduates funded by your agreement who graduated during this period and will receive scholarships or fellowships for further studies in science, mathematics, engineering or technology fields:	0.00

Names of Personnel receiving masters degrees

NAME

Total Number:

Names of personnel receiving PHDs

NAME

Total Number:

Names of other research staff

NAME	PERCENT SUPPORTED

FTE Equivalent:

Total Number:

Sub Contractors (DD882)

Inventions (DD882)

Scientific Progress

See Attachment

Technology Transfer

Development and Application of a Soil Moisture Downscaling Method for Mobility Assessment

Final Report for STIR Grant:
"Evaluation and Application of a Soil Moisture Downscaling Method for Mobility Assessment"

Michael L. Coleman
Jeffrey D. Niemann (Principle Investigator)
Department of Civil and Environmental Engineering
Colorado State University

Contents

Figures

Tables

1. Introduction and Objectives

Soil moisture is a central variable to many activities of the Army. It affects combat logistics including camp siting and troop routing. It impacts the sustainable management of training lands through its association with erosion and land degradation, and it plays a role in target acquisition systems and the detection of improvised explosive devices (IEDs), landmines, and unexploded ordnance. In assessments of vehicle mobility, soil moisture affects the rating cone index, which is used as a measure of soil strength (Mason et al., 2001). As the soil moisture increases, the soil strength and thus the trafficability decrease nonlinearly. When the soil moisture is relatively high, small differences in its value can change the trafficability conditions from "go" to "no go" (Mason and Baylot, 2009). Soil moisture is also a central variable in hydrology. It affects rates of infiltration, evaporation, transpiration, and groundwater recharge, and it controls the partitioning of available energy at the land surface into sensible and latent heat fluxes. For example, antecedent soil moisture conditions have been shown to affect the production of floods and to benefit real-time flood forecasting (Kitanidis and Bras, 1980; Ntelekos et al., 2006).

Unfortunately, soil moisture is difficult to observe directly with the spatial resolutions (grid cells with 10-30 m linear dimensions) and extents (10,000-250,000 ha) that are required for many of the applications described earlier. In-situ measurement techniques such as time-domain reflectometry (TDR) can accurately measure soil moisture over small distances (centimeters) (Noborio, 2001; Robinson et al., 2003), but this method is impractical for estimation of soil moisture over large spatial extents. Alternatively, soil moisture can be inferred using satellite sensors. Satellite-based active/passive radiometers can estimate soil moisture over large spatial extents, but they are only sensitive to soil moisture near the soil surface (top 2-3 cm), and their spatial resolution is typically very coarse (10-25 km) (e.g., Entekhabi et al., 2004). Other methods estimate soil moisture from an energy balance of the land surface, which is inferred from optical and thermal remote-sensing images (Ahmad and Bastiaanssen, 2003; Scott et al., 2003; Fleming et al., 2005). This approach can produce spatial patterns with a 1 km resolution if images are required on any given date (which requires use of the MODIS instrument). In addition, processing of such images is highly technical and thus expensive. Soil moisture can be inferred from weather forecasting models such as the Air Force Weather Agency's (AFWA) Agricultural Meteorology (AGRMET) model (AFWA, 2002), but these models also typically

produce estimates with coarse spatial resolutions (1-40 km). Ground-based methods are being developed to produce soil moisture estimates using cosmic rays (Desilets et al., 2010; Shuttleworth et al., 2010), but these methods still have a relatively coarse resolution (~800 m).

Thus, methods are required to downscale remote-sensing or modeling values from an intermediate resolution of about 1 km to a fine resolution of about 30 m. Such estimation methods require an additional data source that is both available at the fine resolution and strongly related to soil moisture variations. Topographic data is available nearly globally at a 30 m resolution from ASTER (Abrams et al., 2010), and various topographic attributes are known to influence soil moisture patterns at the spatial resolutions of interest (Western et al., 1999; Florinsky et al., 2002; Lin et al., 2006). For example, Burt and Butcher (1985) studied a 1.4 ha hillslope and found that the so-called wetness index explained the accumulation of water at downhill and lower-slope locations at certain times. The wetness index is calculated from the specific contributing area and topographic slope and was originally derived to describe lateral redistribution of water in TopModel (Beven and Kirkby, 1979). Western et al. (1999) observed linear correlations between soil moisture and both the wetness index and the potential solar radiation index (PSRI) in the 10.5 ha Tarrawarra catchment in Australia. PSRI is an index that describes the insolation of a point with a given slope and aspect in comparison to a horizontal surface at the same location (Moore et al., 1993; Dingman, 2002).

Several practical difficulties arise in using topographic information to estimate soil moisture patterns. Within a given region, soil moisture patterns can have different spatial structures at different times (Grayson et al., 1997), and the spatial structures can have complex organizations and discontinuities that are difficult to characterize with standard spatial estimation methods (Fleming et al., 2005). Soil moisture patterns also typically exhibit significant variability across a wide range of spatial scales (Seyfried, 1998; Famiglietti et al., 2008), and the nature of the dependence of soil moisture on topography can be different in different regions (Busch et al., 2011). All of these issues make accurate downscaling or interpolation of soil moisture based on topographic information difficult.

The overall objective of this project is to develop, calibrate, and apply a method to estimate fine-scale soil moisture patterns based on intermediate-resolution soil moisture estimates and the observed topographic dependence of soil moisture. The proposed method is a conceptual model that estimates the local soil moisture based on representations of the processes

that supply or remove water from the soil. These processes include: infiltration, lateral redistribution, deep drainage, and evapotranspiration. The effects of these processes are then calculated using topographic attributes and a supplied spatial-average soil moisture (or a grid of intermediate-resolution soil moisture values).

The outline of this report is as follows. Section 2 derives the conceptual model, and Section 3 describes the implementation of this model in an ArcGIS tool. Section 4 develops two calibrations for the model using two available soil moisture datasets (Tarrawarra and Cache la Poudre). This section also evaluates the performance of the method at these watersheds, and compares the performance to other available methods. Section 5 describes the application of the method to downscale intermediate-resolution soil moisture patterns for selected regions in Afghanistan. This section also compares attributes of the original and downscaled patterns that are relevant for mobility analysis. Finally, Section 6 closes with the conclusions and possible directions for future research.

2. Methodology

In this section, a model is derived that determines the soil moisture at any location within a region if the spatial-average soil moisture is known. The spatial average might be a single value for all locations in the region or a grid of average soil moisture values from remote-sensing or model simulations. The local soil moisture is determined using a steady-state approximation. All processes that affect soil moisture are assumed to occur steadily in time, and the soil moisture is assumed to be at equilibrium so that the total inflow and outflow are balanced. The processes that transport water to or from the soil are infiltration F, deep drainage or recharge to groundwater G, lateral unsaturated flow L, and evapotranspiration E. One can write the water balance for the land area that drains through any given segment of an elevation contour as:

$$\int_0^A F da = \int_0^A G da + L + \int_0^A E da \tag{1}$$

where A is the land area that can contribute flow to the contour segment and F, G, and E are the infiltration, recharge, and evapotranspiration rates within that land area (these are expected to vary spatially). L is the lateral outflow occurring through the contour segment.

The deep drainage at any point is modeled as percolation, which means that the hydraulic gradient is controlled by gravity. Under this assumption, G can be written as:

$$G = K_v \tag{2}$$

where K_v is the unsaturated vertical hydraulic conductivity. Using the Campbell (1974) equation to describe unsaturated hydraulic conductivity, K_v can be written:

$$K_v = K_{s,v}\theta^{\gamma_v} / \phi^{\gamma_v} \tag{3}$$

where $K_{s,v}$ is the vertical saturated hydraulic conductivity, θ is the volumetric soil moisture, ϕ is the porosity, and γ_v is the pore size distribution index. This implies:

$$G = K_{s,v}\theta^{\gamma_v} / \phi^{\gamma_v} \tag{4}$$

Lateral flow at any location is described using Darcy's Law and assuming uniform flow with depth in the soil. Using this approach, the lateral flow is:

$$L = -\delta c K_h S \tag{4}$$

where δ is the depth within which lateral flow occurs (assumed to be the soil depth), c is the length of the contour segment being considered (in practice, the linear dimension of a fine-resolution grid cell), K_h is the unsaturated horizontal hydraulic conductivity, and S is the hydraulic gradient in the horizontal direction. Heimsath et al. (1999) found that soil depth δ depends linearly on the topographic curvature:

$$\delta = \delta_0(\kappa_{\min} - \kappa) / \kappa_{\min} \tag{6}$$

where δ_0 is the soil depth when the curvature is zero and $\kappa_{\min}$ is the minimum curvature for which soil is present. Note that curvature is defined as positive for convergent locations and negative for divergent locations. Using this expression for soil depth and the Campbell (1974) equation for unsaturated hydraulic conductivity, the lateral flow can be written:

$$L = -\delta_0\left(\frac{\kappa_{\min} - \kappa}{\kappa_{\min}}\right) c K_{s,h} \frac{\theta^{\gamma_h}}{\phi^{\gamma_h}} S \tag{7}$$

where $K_{s,h}$ is the horizontal saturated hydraulic conductivity and γ_h is the pore size distribution index in the horizontal direction.

Evapotranspiration (ET) is determined as a function of a local potential evapotranspiration (PET), which is denoted E_p^*. The local PET is calculated from the Penman combination equation (Chow et al., 1988):

$$E_p^* = \left[\frac{\Delta}{\Delta + \Gamma} E_r PSRI + \frac{\Delta}{\Delta + \Gamma} E_a\right] \tag{5}$$

where Δ is rate of change of saturation vapor pressure with air temperature, Γ is the psychrometric constant, E_r is the ET due to radiation, and E_a is the aerodynamic or humidity-based ET. *PSRI* is the potential solar radiation index, which is the ratio between the insolation of the topographic surface relative to that of a horizontal surface at the same location. The *PSRI* can be calculated as a function of the day of year, latitude and topographic slope and aspect (Western et al., 1999; Dingman, 2002). This equation implicitly neglects sensible and ground heat fluxes in the energy balance estimate by including *PSRI* as shown above. The Priestley-Taylor equation (Chow et al., 1988) assumes that the humidity-based term is a specified fraction α of the radiation-based term, which implies:

$$E_p^* = \left[\frac{\Delta}{\Delta + \Gamma} E_r PSRI + \alpha \frac{\Delta}{\Delta + \Gamma} E_r \right] \tag{9}$$

A PET can be similarly calculated for the entire region (denoted E_p). Over large areas, the impact of the topography on the insolation is usually neglected, and the Priestley-Taylor equation implies a regional PET:

$$E_p = \left[\frac{\Delta}{\Delta + \Gamma} E_r + \alpha \frac{\Delta}{\Delta + \Gamma} E_r \right] \tag{10}$$

Combining Equations (9) and (10), one can write the local PET in terms of the regional Priestly-Taylor PET:

$$E_p^* = \frac{E_p PSRI}{1+\alpha} + \frac{E_p \alpha}{1+\alpha} \tag{11}$$

The actual evapotranspiration E is then calculated by accounting for the effects of moisture limitations, which is modeled with power functions as shown below:

$$E = \frac{E_p PSRI}{1+\alpha} \left(\frac{\theta}{\phi} \right)^{\beta_r} + \frac{E_p \alpha}{1+\alpha} \left(\frac{\theta}{\phi} \right)^{\beta_a} \tag{12}$$

where β_r and β_a are vegetation-related parameters. Based on the literature (Entekhabi et al., 1991; Rodriguez-Iturbe et al., 1991), a single β would be applied to both terms in Equation (12). Here, we allow distinct exponents because moisture limitations may affect the radiation-based and humidity-based terms in different ways.

We now substitute the expressions for *G*, *L*, and *E* from Equations (4), (7), and (12) back into Equation (1), which produces:

$$\int_0^A F da = \frac{K_{s,v}}{\phi^{\gamma_v}} \int_0^A \theta^{\gamma_v} da - \frac{\delta_0(\kappa_{\min} - \kappa) K_{s,h}}{\kappa_{\min} \phi^{\gamma_h}} cS\theta^{\gamma_h} + \frac{E_p}{(1+\alpha)\phi^{\beta_r}} \int_0^A PSRI\,\theta^{\beta_r} da + \frac{E_p \alpha}{(1+\alpha)\phi^{\beta_a}} \int_0^A \theta^{\beta_a} da \quad (13)$$

In this expression, we have assumed that ϕ, $K_{s,v}$, $K_{s,h}$, γ_v, γ_h, δ_0, $\kappa_{\min}$, α, β_r, β_a, and E_p are all spatially constant. Similar to TopModel (Beven and Kirkby, 1979), the infiltration rate is also assumed to be spatially constant, and the hydraulic gradient is assumed to be equal to minus the local topographic slope S. Thus, the equation becomes:

$$F = \frac{K_{s,v}}{\phi^{\gamma_v} A} \int_0^A \theta^{\gamma_v} da + \frac{\delta_0(\kappa_{\min} - \kappa) K_{s,h}}{\kappa_{\min} \phi^{\gamma_h} A} cS\theta^{\gamma_h} + \frac{E_p}{(1+\alpha)\phi^{\beta_r} A} \int_0^A PSRI\,\theta^{\beta_r} da + \frac{E_p \alpha}{(1+\alpha)\phi^{\beta_a} A} \int_0^A \theta^{\beta_a} da \quad (14)$$

An explicit, analytical solution cannot be obtained for Equation (14), so an approximate solution is developed by first considering four simplified cases where one of the four terms on the right (deep drainage, lateral outflow, radiation-based ET or humidity-based ET) is much more important than the others. If deep drainage dominates, Equation (14) can be approximated:

$$F = \frac{K_{s,v}}{\phi^{\gamma_v} A} \int_0^A \theta^{\gamma_v} da \quad (15)$$

In this case, water movement between locations is negligible, so the infiltration at any point in the catchment must balance the deep drainage at that point. Therefore, the water balance equation can be written locally as:

$$F = \frac{K_{s,v}}{\phi^{\gamma_v}} \theta^{\gamma_v} \quad (16)$$

Solving for soil moisture, one obtains:

$$\theta = \phi \left(\frac{F}{K_{s,v}} \right)^{1/\gamma_v} \quad (17)$$

The initial objective was to determine the local soil moisture θ as a function of an available spatial-average soil moisture $\bar{\theta}$. $\bar{\theta}$ can be calculated by integrating Equation (17) over the region for which $\bar{\theta}$ is available. If A_p is defined as the area of this region, the spatial average is:

$$\bar{\theta} = \frac{1}{A_p} \int \theta \, da \quad (18)$$

Substituting Equation (17) into Equation (18) and noting that all of the terms that determine θ are spatially constant, one obtains:

$$\bar{\theta} = \phi \left(\frac{F}{K_{s,v}} \right)^{1/\gamma_v} \tag{19}$$

Comparing this expression with Equation (17), one observes that:

$$\theta = \bar{\theta} \tag{20}$$

Thus, the soil moisture is spatially uniform if deep drainage is the dominant outflow process.

We now consider the second case where lateral drainage is the dominant outflow process. In this case, Equation (14) simplifies to:

$$F = \frac{\delta_0 (\kappa_{\min} - \kappa) K_{s,h}}{\kappa_{\min} \phi^{\gamma_h} A} cS\theta^{\gamma_h} \tag{21}$$

Solving for θ, one obtains:

$$\theta = \phi \left(\frac{F}{\delta_0 K_{s,h}} \right)^{1/\gamma_h} \left(\frac{A}{cS} \right)^{1/\gamma_h} \left(\frac{\kappa_{\min}}{\kappa_{\min} - \kappa} \right)^{1/\gamma_h} \tag{22}$$

Integrating Equation (22) over the region for which a spatial average is available, one obtains:

$$\bar{\theta} = \frac{1}{A_p} \int_{A_p} \theta da = \phi \left(\frac{F}{\delta_0 K_{s,h}} \right)^{1/\gamma_h} \frac{1}{A_p} \int \left(\frac{A}{cS} \right)^{1/\gamma_h} \left(\frac{\kappa_{\min}}{\kappa_{\min} - \kappa} \right)^{1/\gamma_h} da \tag{23}$$

The term that remains in the integral $(A/cS)^{1/\gamma_h} \left[\kappa_{\min} / (\kappa - \kappa_{\min}) \right]^{1/\gamma_h}$ is a compound topographic index, which we call the lateral flow index (LFI). The average LFI within the region is denoted Λ, and it is:

$$\Lambda = \frac{1}{A_p} \int \left(\frac{A}{cS} \right)^{1/\gamma_h} \left(\frac{\kappa_{\min}}{\kappa_{\min} - \kappa} \right)^{1/\gamma_h} da \tag{24}$$

Substituting this equation back into Equation (23), one obtains:

$$\bar{\theta} = \phi \left(\frac{F}{\delta_0 K_{s,h}} \right)^{1/\gamma_h} \Lambda \tag{25}$$

Combining Equations (22) and (25), one gets:

$$\theta = \frac{\bar{\theta}}{\Lambda} \left(\frac{A}{cS} \right)^{1/\gamma_h} \left(\frac{\kappa_{\min}}{\kappa_{\min} - \kappa} \right)^{1/\gamma_h} \tag{26}$$

Thus, the spatial pattern of soil moisture is determined by spatial variations in the LFI if lateral flow dominates.

Next, we consider the case where the radiation-based ET term in Equation (14) is dominant. Under this scenario, one can simplify the equation as:

$$F = \frac{E_p}{(1+\alpha)\phi^{\beta_r} A}\int_0^A PSRI\,\theta^{\beta_r}\,da \tag{27}$$

Again, noting that water movement between locations is negligible in this case, one can rewrite Equation (28) as a local water balance:

$$F = \frac{E_p}{(1+\alpha)\phi^{\beta_r}} PSRI\,\theta^{\beta_r} \tag{28}$$

Solving for θ, one obtains:

$$\theta = \phi\left(\frac{F(1+\alpha)}{E_p}\right)^{1/\beta_r}\left(\frac{1}{PSRI}\right)^{1/\beta_r} \tag{29}$$

Integrating over the region to calculate the spatial-average soil moisture, one gets:

$$\bar{\theta} = \frac{1}{A_p}\int \theta da = \phi\left(\frac{F(1+\alpha)}{E_p}\right)^{1/\beta_r}\frac{1}{A_p}\int\left(\frac{1}{PSRI}\right)^{1/\beta_r} da = \phi\left(\frac{F(1+\alpha)}{E_p}\right)^{1/\beta_r}\Pi \tag{30}$$

where Π is the average of an evapotranspiration index (ETI), which is defined as $(1/PSRI)^{1/\beta_r}$. Combining Equations (29) and (30), one gets:

$$\theta = \frac{\bar{\theta}}{\Pi}\left(\frac{1}{PSRI}\right)^{1/\beta_r} \tag{31}$$

Thus, if the radiation-based ET term dominates the water balance, the spatial pattern of soil moisture is determined by the spatial variations of the ETI.

Finally, we consider the case where the humidity-related ET term dominates. In this case, Equation (14) can be written:

$$F = \frac{E_p\alpha}{(1+\alpha)\phi^{\beta_a} A}\int_0^A \theta^{\beta_a}\,da \tag{32}$$

Water movement between locations is negligible in this case, so one can rewrite Equation (32) as a local water balance:

$$F = \frac{E_p\alpha}{(1+\alpha)\phi^{\beta_a}}\theta^{\beta_a} \tag{33}$$

Solving for θ, one obtains:

$$\theta = \phi\left(\frac{F(1+\alpha)}{E_p\alpha}\right)^{1/\beta_a} \tag{34}$$

Integrating over the region to calculate the spatial-average soil moisture, one finds:

$$\overline{\theta} = \frac{1}{A_p}\int \theta da = \phi\left(\frac{F(1+\alpha)}{E_p\alpha}\right)^{1/\beta_a} \tag{35}$$

Combining Equations (34) and (35), one gets:

$$\theta = \overline{\theta} \tag{36}$$

Four estimates for the soil moisture have been produced depending on whether deep drainage, lateral flow, radiation-based ET, or humidity-based ET is the dominant process. These estimates are

$$\theta_G = \overline{\theta} \tag{37}$$

and:

$$\theta_L = \frac{\overline{\theta}}{\Lambda}\left(\frac{A}{cS}\right)^{1/\gamma_h}\left(\frac{\kappa_{\min}}{\kappa_{\min}-\kappa}\right)^{1/\gamma_h} \tag{38}$$

and:

$$\theta_R = \frac{\overline{\theta}}{\Pi}\left(\frac{1}{PSRI}\right)^{1/\beta_r} \tag{39}$$

and:

$$\theta_A = \overline{\theta} \tag{40}$$

A final estimate for θ is obtained using a weighted, arithmetic average of these four approximations:

$$\theta = \frac{w_G\theta_G + w_L\theta_L + w_R\theta_R + w_A\theta_A}{w_G + w_L + w_R + w_A} \tag{41}$$

where w_G, w_L, w_R, w_A are the weights. One expects the weights to depend on the magnitude of the terms associated with the processes in Equation (14). In particular, the weight for the deep drainage estimate w_G should be large if the deep drainage term in Equation (14) is large. Thus, it is proposed that:

$$w_G = \frac{K_{s,v}}{\phi^{\gamma_v}A}\int_0^A \theta^{\gamma_v} da \tag{42}$$

However, this equation is not easily evaluated because it includes the average soil moisture for the area upslope from the contour segment being considered. If this average is approximated with the local soil moisture estimate θ_G in Equation (37), then Equation (42) becomes:

$$w_G = \frac{K_{s,v}}{\phi^{\gamma_v}} \overline{\theta}^{\gamma_v} \tag{43}$$

Similarly, the weight for the lateral flow estimate can be estimated from the associated term in Equation (14):

$$w_L = \frac{\delta_0(\kappa_{\min} - \kappa)K_{s,h}}{\kappa_{\min}\phi^{\gamma_h} A} cS\theta^{\gamma_h} \tag{44}$$

If θ is approximated with the estimate θ_L in Equation (38), then Equation (44) becomes:

$$w_L = \delta_0 K_{s,h} \left(\frac{\overline{\theta}}{\phi\Lambda} \right)^{\gamma_h} \tag{45}$$

The weight for the radiation-based ET term is:

$$w_R = \frac{E_p}{(1+\alpha)\phi^{\beta_r} A} \int_0^A PSRI\theta^{\beta_r} da \tag{46}$$

Notice that this expression includes the average of $PSRI\theta^{\beta_r}$ for the region upslope of the contour segment. Approximating this average with the local soil moisture estimate θ_R, one obtains:

$$w_R = \frac{E_p}{1+\alpha} \left(\frac{\overline{\theta}}{\phi\Pi} \right)^{\beta_r} \tag{47}$$

Finally, the weight for the humidity-related ET term is:

$$w_A = \frac{E_p \alpha}{(1+\alpha)\phi^{\beta_a} A} \int_0^A \theta^{\beta_a} da \tag{48}$$

Replacing the average of θ^{β_a} in this expression with the estimate of the local soil moisture θ_A, one obtains:

$$w_A = \frac{E_p \alpha}{1+\alpha} \left(\frac{\overline{\theta}}{\phi} \right)^{\beta_a} \tag{49}$$

Equations (37), (38), (39), (40), (43), (45), (47), and (49), are now substituted into Equation (41), and one obtains:

$$\theta = \frac{K_{s,v}\left(\frac{\bar{\theta}}{\phi}\right)^{\gamma_v}\bar{\theta} + \delta_0 K_{s,h}\left(\frac{\bar{\theta}}{\phi\Lambda}\right)^{\gamma_h}\left[\frac{\bar{\theta}}{\Lambda}\left(\frac{A}{cS}\right)^{1/\gamma_h}\left(\frac{\kappa_{\min}}{\kappa_{\min}-\kappa}\right)^{1/\gamma_h}\right] + \frac{E_p}{1+\alpha}\left(\frac{\bar{\theta}}{\phi\Pi}\right)^{\beta_r}\left[\frac{\bar{\theta}}{\Pi}\left(\frac{1}{PSRI}\right)^{1/\beta_r}\right] + \frac{E_p\alpha}{1+\alpha}\left(\frac{\bar{\theta}}{\phi}\right)^{\beta_a}\bar{\theta}}{K_{s,v}\left(\frac{\bar{\theta}}{\phi}\right)^{\gamma_v} + \delta_0 K_{s,h}\left(\frac{\bar{\theta}}{\phi\Lambda}\right)^{\gamma_h} + \frac{E_p}{1+\alpha}\left(\frac{\bar{\theta}}{\Pi\phi}\right)^{\beta_r} + \frac{E_p\alpha}{1+\alpha}\left(\frac{\bar{\theta}}{\phi}\right)^{\beta_a}} \quad (50)$$

which is the equation that is used to downscale the soil moisture patterns. In the end, the local soil moisture is estimated from the contributions of four terms. The deep drainage and humidity-related ET terms do not produce any spatial variability. The spatial variability due to lateral flow is introduced by the LFI, which depends on the parameters γ_h and $\kappa_{\min}$, and the spatial variability due to radiation-related ET is introduced by the ETI, which depends on one parameter β_r. The importance of each of these patterns is determined by the weights, which depend on the spatial-average soil moisture $\bar{\theta}$ and various parameters. The general structure of weighting topographic-based patterns using coefficients that depend on $\bar{\theta}$ is similar to the empirical orthogonal function (EOF) approach that was used by Perry and Niemann (2007, 2008). In that approach, the patterns of spatial variation are the EOFs, which are estimated from empirical relationships to topographic attributes. The importance of these patterns on any given date is determined by the associated expansion coefficients, which are estimated as a function of $\bar{\theta}$. The structure is also similar to the dynamic linear regression model that was proposed by Wilson et al. (2005). In that method, the soil moisture is estimated by linear regressions against topographic attributes, but the regression coefficients are adjusted based on the spatial-average soil moisture. Like the EOF method, the Wilson et al. (2005) method is empirical.

3. Software Implementation

The derived model was implemented using the Matlab® (Mathworks, 2009) and ArcMap® (ESRI, 2006) software packages. The model calculations were written as a Matlab® script and exported as an executable program that is called by the GIS tool. Instructions for installing and using the GIS tool are provided in the user manual (Coleman et al., 2011). Although technically not required for use of the model, the TauDEM toolbox for GIS can be used to calculate the slope and contributing area topographic attributes (Tarboton et al., 1997), which are required by the conceptual model. TauDEM is a free, open-source software package and instructions for obtaining it are provided in the user manual (Coleman et al., 2011).

Although the full model is presented in Equation (50), several simplifications were made in the current GIS implementation. First, the porosity ϕ is given a pre-specified value of 0.5 because tests of early versions of the model indicated that it had sufficient flexibility from other parameters so that its performance was not reduced by doing so. In addition, fixing this parameter in advance helps the parameter optimization method converge more quickly. Second, the pore-size distribution indices γ_h and γ_v were assumed to be equal, leading to a single γ parameter for both the horizontal and vertical directions. Third, the α parameter, which determines the humidity-based ET as a fraction of the radiation-based ET, was chosen to be 0. This assumption presumes the dominance of radiation in determining ET, and it removes the β_a parameter from the current implementation, so only a single β is required. The net effect of these simplifications is to reduce the total number of parameters from 10 to 6.

4. Model Calibration

The model was calibrated and tested at two different catchments, the Tarrawarra catchment near Melbourne, Australia (Western and Grayson, 1998) and a research catchment in the Cache la Poudre river basin in northern Colorado (Lehman and Niemann, 2009). The Tarrawarra catchment has homogeneous pasture vegetation, a temperate climate, moderately deep soils, and moderate rolling topography. The Cache la Poudre catchment has aspect-dependent forest and shrub vegetation, a semi-arid climate, shallow soil with rocky outcrops, and steep mountainous topography. The different climates of the catchments are reflected in the distinct ranges of $\bar{\theta}$ for the soil moisture datasets at each catchment (Figure 1). At the Tarrawarra catchment, soil moisture data were collected on 13 dates in the period between September 1995 and November 1996. The soil moisture data for the Cache la Poudre catchment were collected on 9 dates between April and June 2008.

The calibration of the model at each catchment utilized all of that catchment's soil moisture data. Specifically, a single parameter set was determined for all dates at each catchment. When applying the model to these catchments (and Afghanistan later in this report), the annual average PET was used for E_p, and the PSRI from the winter solstice was used for *PSRI* in Equation (50). Those choices are consistent with the equilibrium assumption under which the model was developed and were found to perform as good or better than using the

values associated with each date in the dataset. The annual average PET at Tarrawarra is 2.27 mm/day, at the Poudre site it is 2.41 mm/day, and for the region modeled in Afghanistan it is 4.86 mm/day. The model performance was quantified using the Nash-Sutcliffe Coefficient of Efficiency (NSCE), which is given by the following formula:

$$NSCE = 1 - \frac{\sum\left[\theta_{obs} - \theta_{est}\right]^2}{\sum\left[\theta_{obs} - \bar{\theta}_{obs}\right]^2} \tag{51}$$

where θ_{obs} is the observed soil moisture at a location, θ_{est} is the estimated soil moisture at that location (from Equation (50)), and $\bar{\theta}_{obs}$ is the observed spatial-average soil moisture, which is also used as $\bar{\theta}$ in Equation (50). Generally, the best possible value of NSCE is 1. However, Busch et al. (2011) showed that about 40% of the variation in these soil moisture patterns is uncorrelated noise, which makes 0.60 approximately the best value that can be achieved in practice for these datasets. The performance of the calibrated model on each day for the two sites is shown in Figure 1.

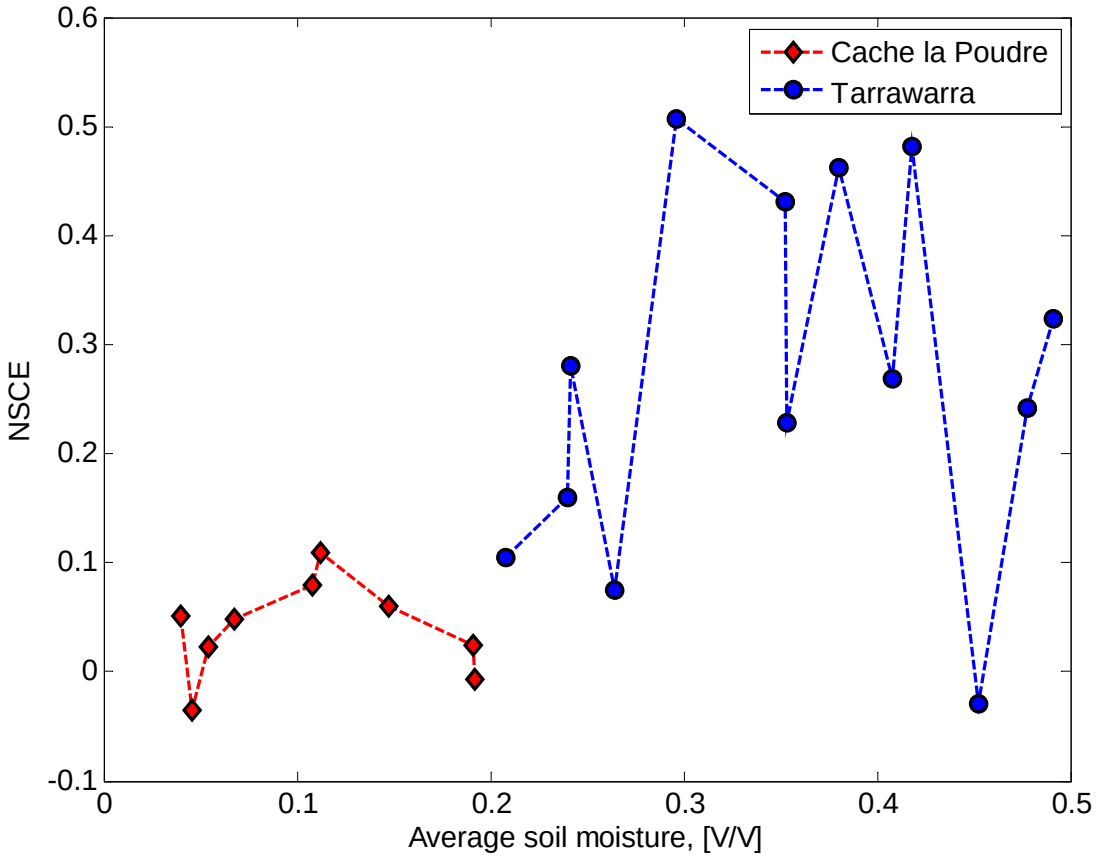

Figure 1 – NSCE results for the soil moisture patterns estimated on all available dates at the Tarrawarra and Cache la Poudre catchments

Note that the average soil moisture values for the two sites do not overlap, but together they represent a range of approximately [0.05, 0.50]. The mean NSCE values are 0.272 and 0.039 for Tarrawarra and Cache la Poudre, respectively. These values are lower than those obtained using the EOF method (Busch et al., 2011), which are 0.348 and 0.140 for Tarrawarra and Cache la Poudre, respectively. However, the model has a greater potential for improvement, for example, by calibrating all 10 parameters. In addition, the model is more readily transferred between sites (Busch et al., 2011). Although the mean NSCE is higher at Tarrawarra, the variability of soil moisture is much lower at the Cache la Poudre catchment, which makes higher NSCE values more difficult to achieve. In addition, the Cache la Poudre catchment has organized, heterogeneous vegetation, which is not considered by the model. The calibrated parameter values from each catchment are listed in Table 1. The associated GIS tool uses the parameter values from Tarrawarra as default values.

Table 1 - Calibrated parameter values

	$K_{s,v}$ mm/day	$K_{s,h}$ mm/day	γ -	ϕ m^3/m^3	δ_0 m	β -	κ_{min} m^{-1}
Tarrawarra	1.913	944.8	5.842	0.5000	0.9651	4.134	-0.3743
Cache la Poudre	11.65	207.9	9.901	0.5000	0.2926	8.690	-0.2048

The LFI and ETI patterns for each catchment are shown in Figure 2. Example observed and estimated moisture patterns as well as the associated residual patterns for Tarrawarra and Cache la Poudre are provided in Figures 3 and 4, respectively. The three scenarios labeled (a), (b) and (c) in each Figures 3 and 4 represent dry, moderate, and wet conditions relative to the range of spatial average moisture values observed at each site. The LFI pattern is evident in the observed moderate soil moisture pattern as well as in the estimated patterns for all conditions at Tarrawarra. This results from the strong influence of lateral flow in determining the soil moisture patterns at this catchment. In contrast, none of the observed patterns at the Cache la Poudre catchment exhibit such a marked LFI emphasis. Such a pattern is slightly visible in the

estimated patterns at Cache la Poudre but less so than at Tarrawarra. That result is due to the stronger influence of ET on the moisture patterns at Cache la Poudre.

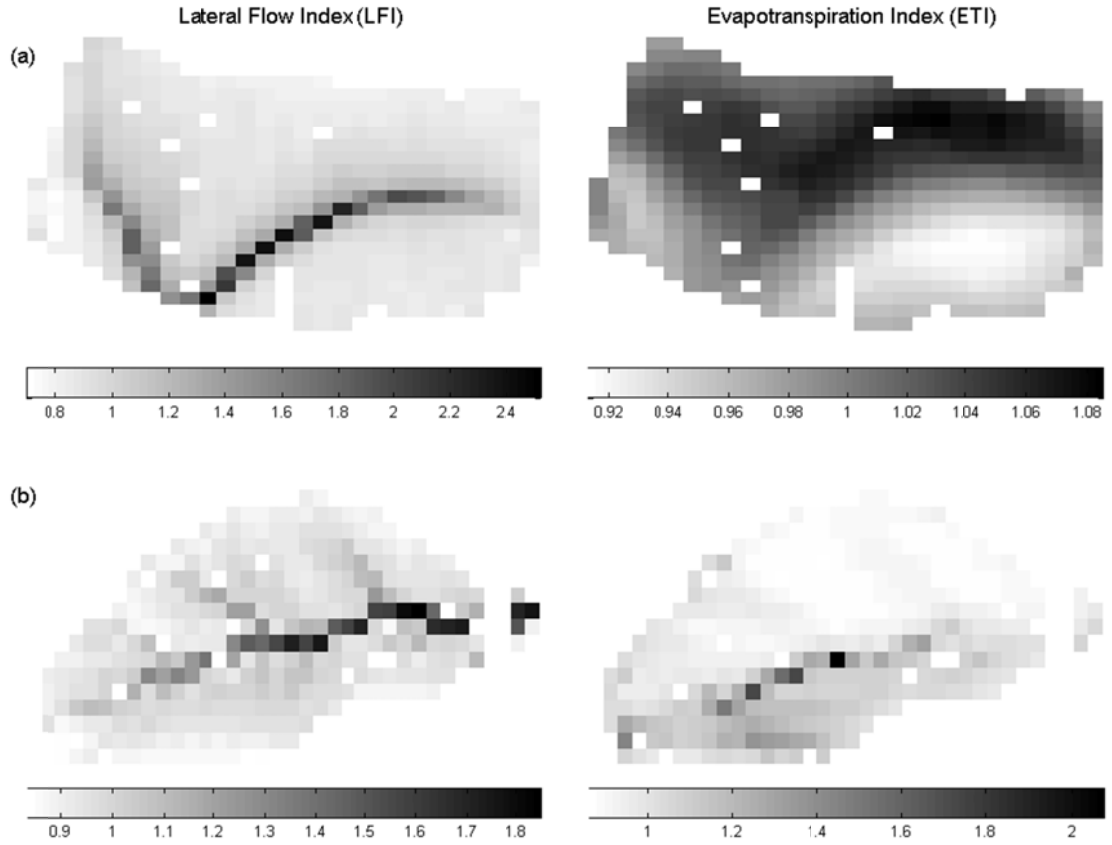

Figure 2 - Lateral flow index (LFI) and evapotranspiration index (ETI) patterns for the (a) Tarrawarra and (b) Cache la Poudre catchments

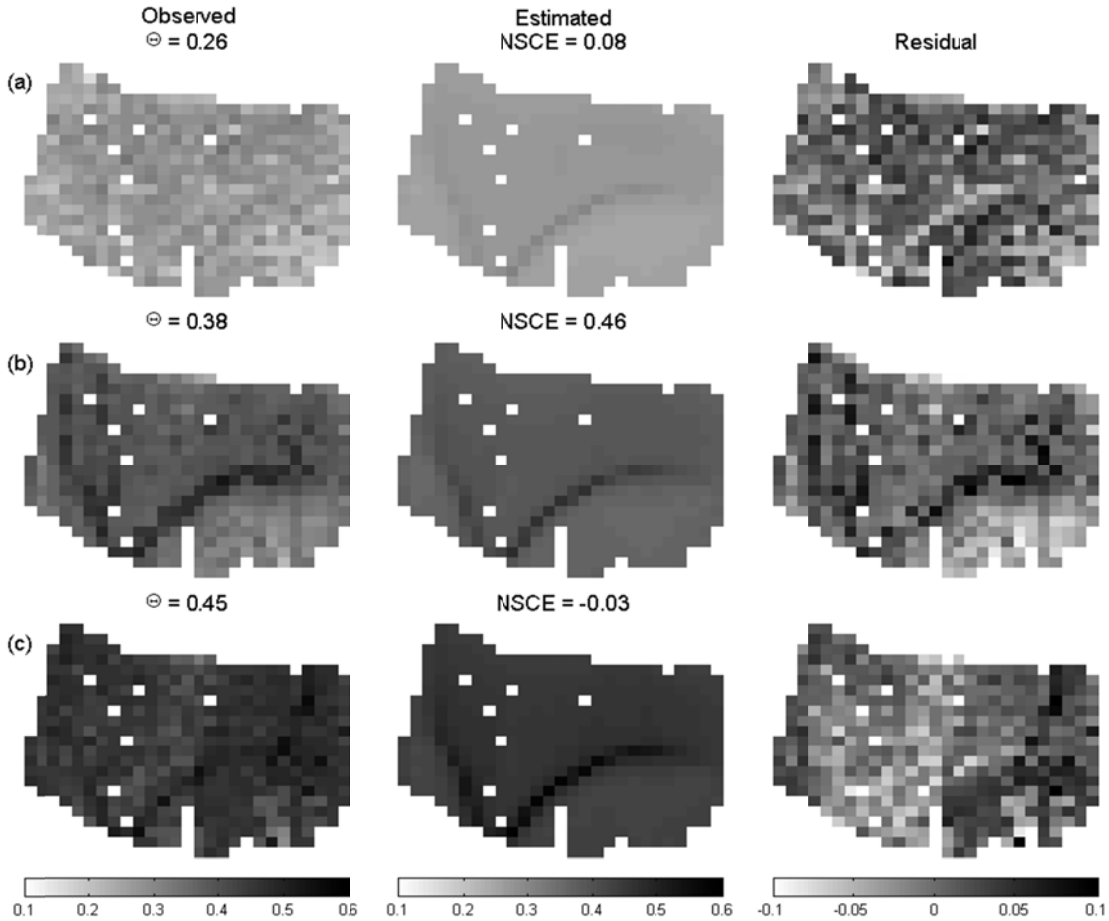

Figure 3 – Examples of observed and estimated patterns for the Tarrawarra catchment under (a) dry, (b) moderate, and (c) wet conditions

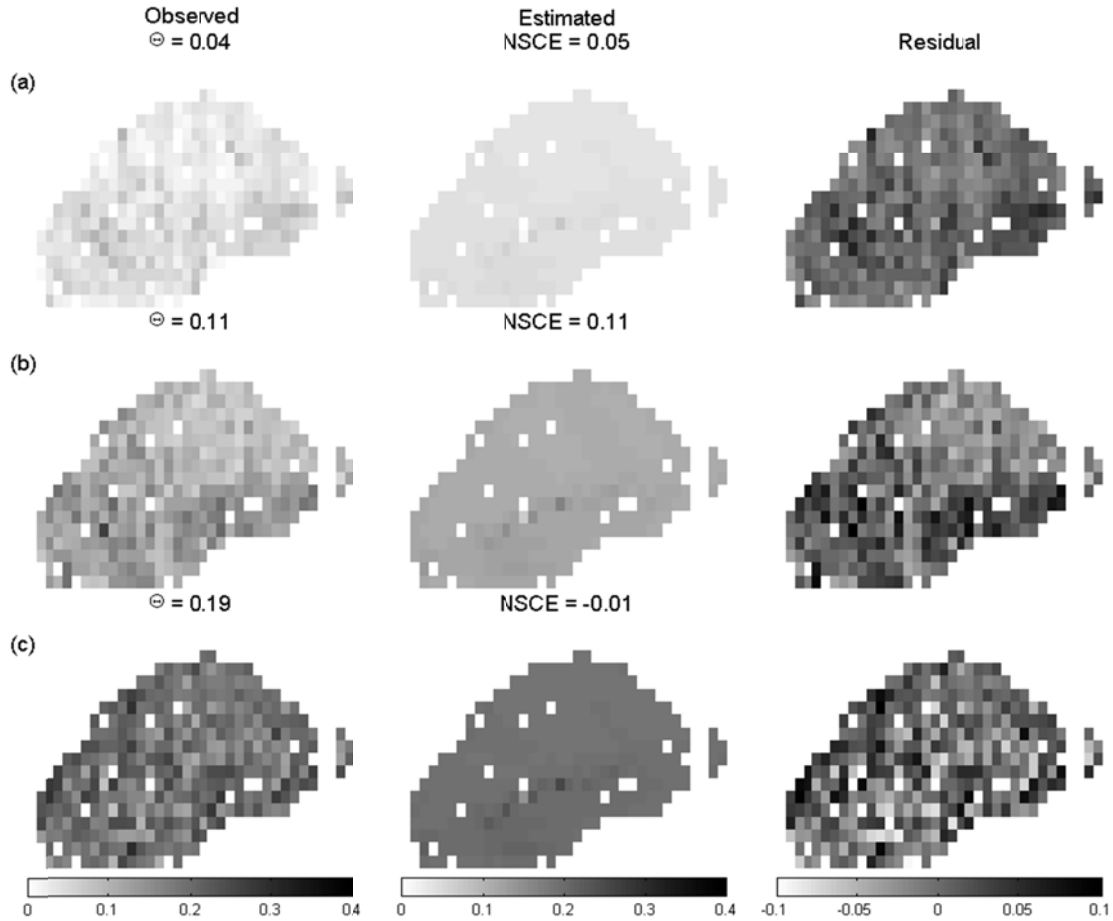

Figure 4 – Examples of observed and estimated patterns for the Cache la Poudre catchment under (a) dry, (b) moderate, and (c) wet conditions

5. Model Application

The calibrations of the model were used to downscale intermediate resolution (1 km) soil moisture datasets representing dry, wet, and very wet conditions for approximately a 50 km by 50 km region near Farah, Afghanistan. The intermediate resolution soil moisture data were originally generated by running the AFWA model over the Afghanistan region. The downscaling model was applied using topographic attributes calculated from the ASTER digital elevation model (DEM) of the region with an approximate resolution of 30 m. Each value from the intermediate resolution soil moisture pattern was used as the average soil moisture value for that pixel in the downscaling method. The dry condition was downscaled using the parameters calibrated for the Cache la Poudre catchment because that dataset includes spatial average soil moisture values similar to the dry condition. The wet and very wet conditions were downscaled

using the parameters from the Tarrawarra catchment because that dataset has spatial average soil moisture values more similar to these cases.

The initial patterns, the downscaled patterns, and the histograms of soil moisture values for each case before and after downscaling are provided in Figures 5, 6, and 7. Figure 8 collects the results from the dry and very wet conditions into a single figure and zooms in to a sub-region, which makes the texture that is imposed by the downscaling method more visible.

In Figure 5, the dry condition, little variation is visible in the downscaled pattern. That result occurs because less variation is produced in the estimated values relative to the other two conditions and because a single color scale is used for all three figures. The low variation in the dry pattern arises in part because only two soil moisture values, 0.07 and 0.11, are present in the intermediate resolution pattern. The histogram indicates that the range of values in the downscaled pattern has two peaks centered on each of the intermediate pattern values. Greater variation is present in the wet and very wet conditions for the intermediate resolution patterns and the downscaled patterns owing to the greater variability in the intermediate resolution moisture values.

The north sides of hillslopes are generally estimated as wetter than the south sides. This is a result of the ETI, which suggests that lower insolation occurs on north-facing slopes. Although difficult to observe in Figures 5 through 7, the effect is more evident in the magnified images in Figure 8. Some points with high estimated moisture values due to this insolation effect are actually too steep to realistically maintain soil. Further refinements of the model can address such situations.

Drainage patterns are also visible in the magnified image of Figure 8 for the very wet condition due to higher moisture estimates in valley bottoms. That feature is due to greater emphasis on the LFI pattern in the model for that situation than in the dry condition. However, discontinuities in the estimates are also apparent in the magnified images. That effect is related to differences in adjacent intermediate resolution values and to different distributions of the topographic attributes within the intermediate resolution pixels.

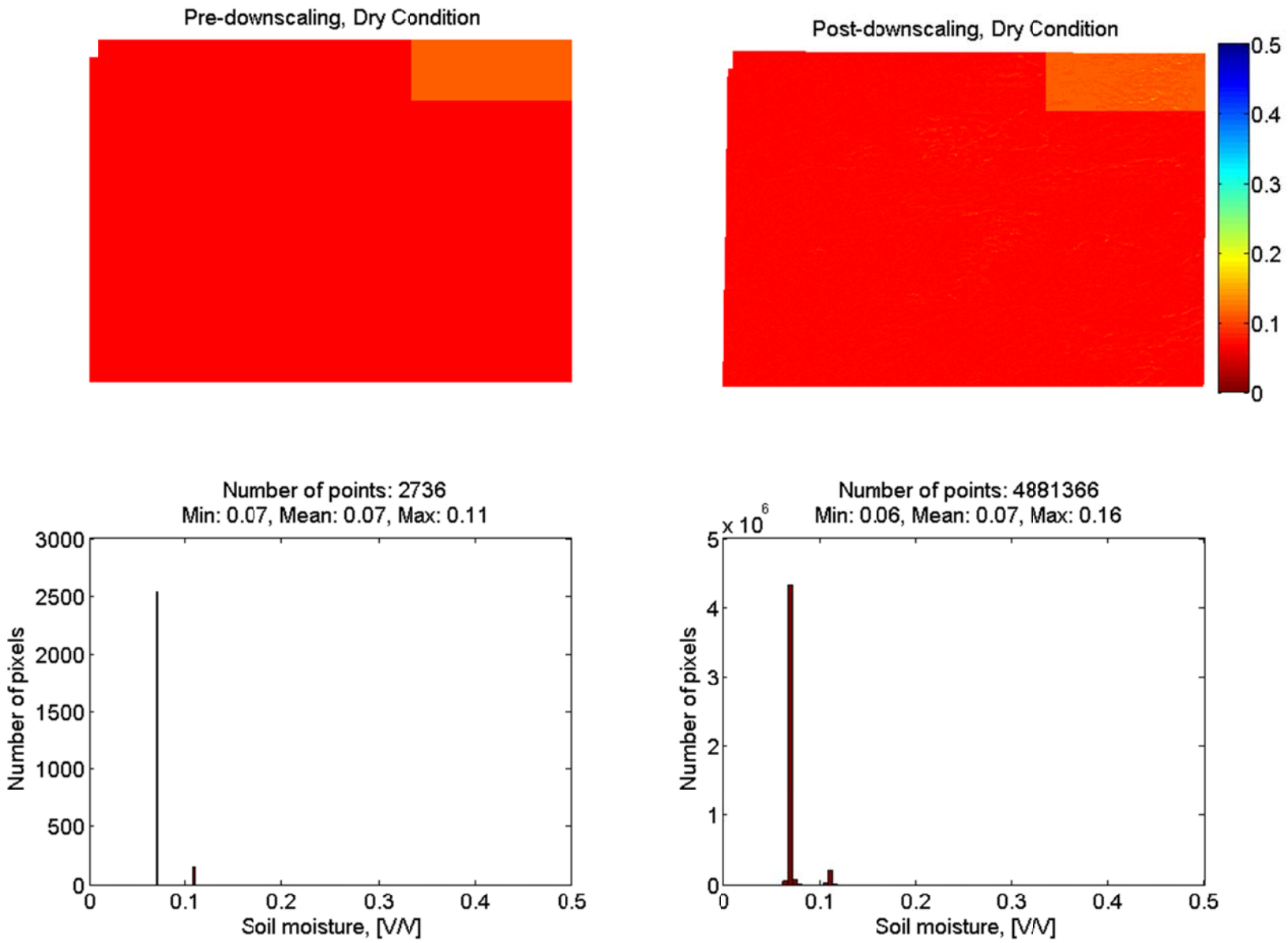

Figure 5 - Patterns and histograms of soil moisture in the Farah region during the dry condition

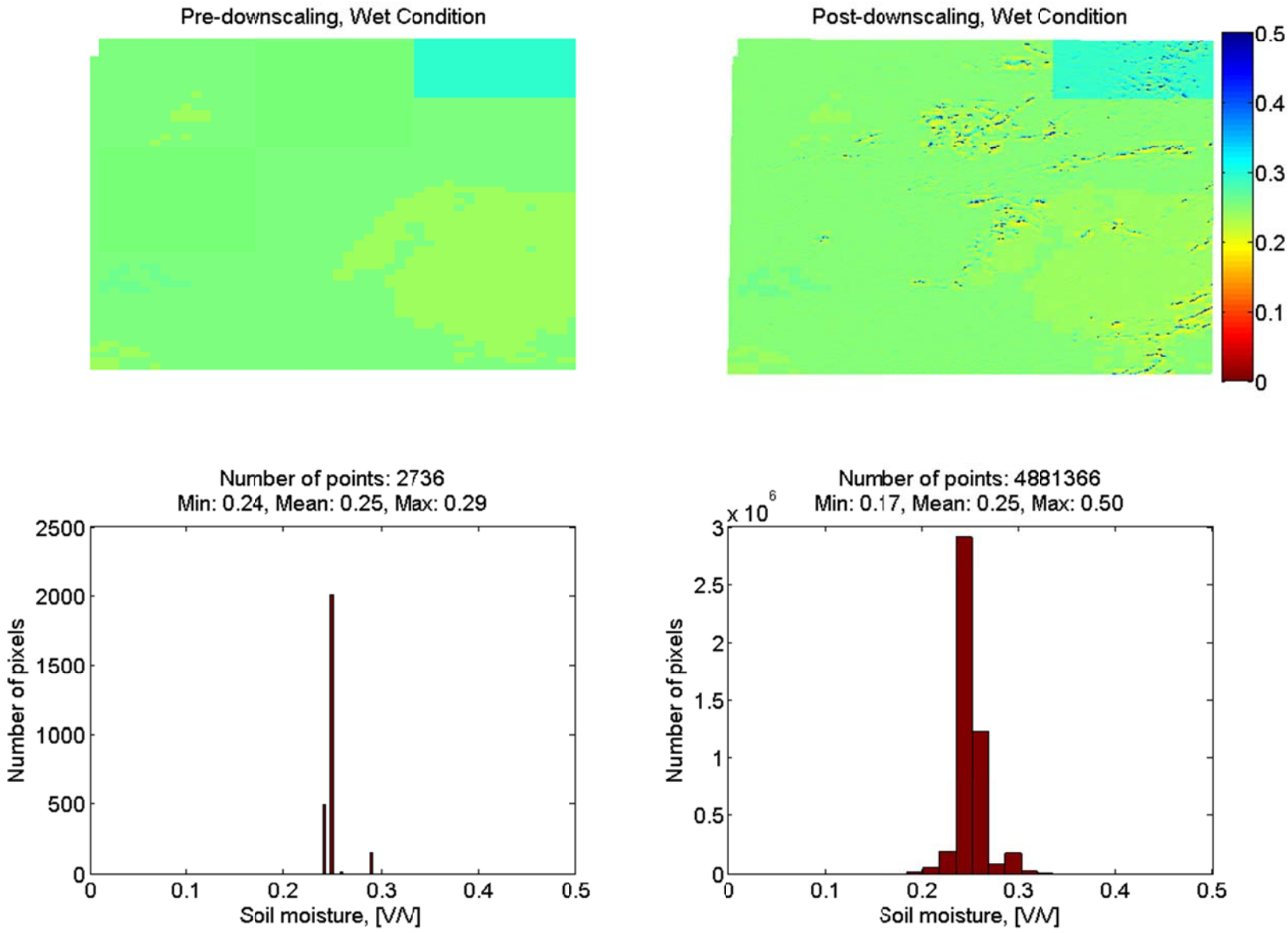

Figure 6 - Patterns and histograms of soil moisture in the Farah region during the wet condition

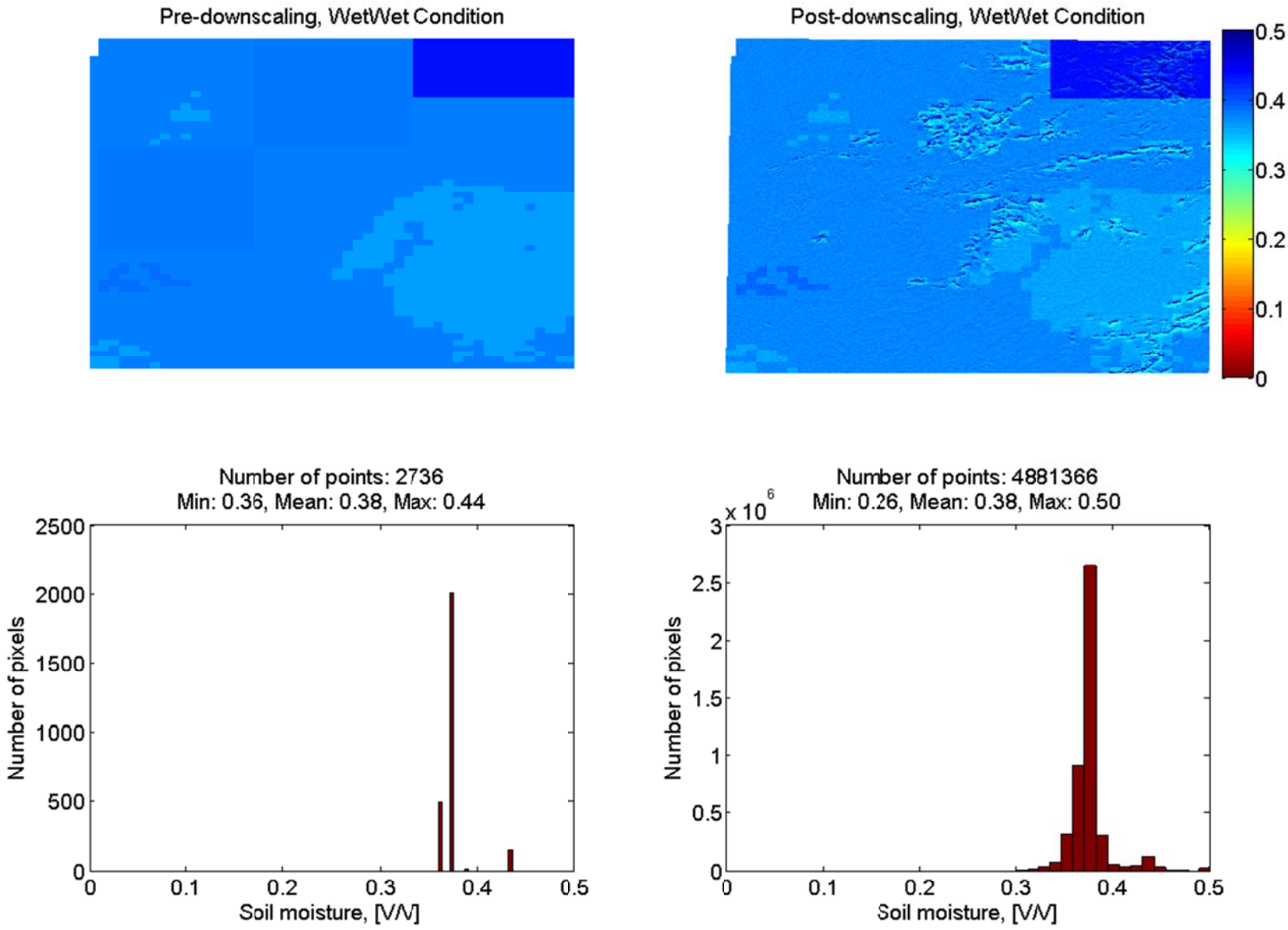

Figure 7 - Patterns and histograms of soil moisture in the Farah region during the very wet condition

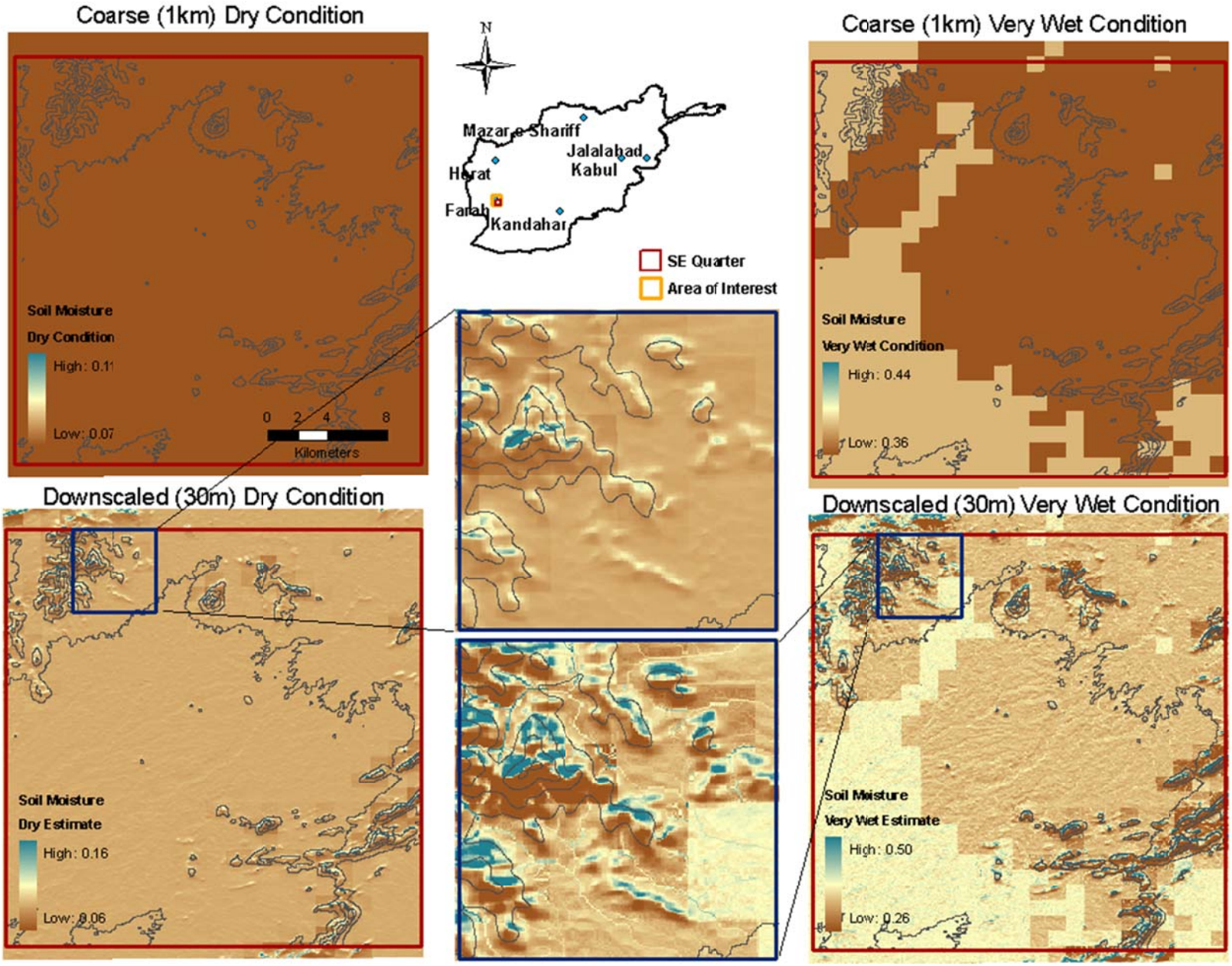

Figure 8 - Magnified soil moisture patterns for the dry and very wet conditions

The model is designed so that the average of the downscaled soil moisture values within any intermediate resolution pixel reproduces the intermediate resolution value exactly. However, that feature can lead to soil moisture values that are greater than the porosity. In reality, such points would be saturated and potentially ponded. The GIS tool contains an option that allows the user to cap the soil moisture values at the porosity value. For the examples presented here, the soil moisture values were limited to 0.50, which is the porosity value used in the model. Capping the soil moisture value at the porosity prevents exact replication of the intermediate resolution pixel values. However, in the cases shown here, the error in the mean is minimal. Alternatively, the estimated soil moisture values could be maintained, and any locations with values greater than the porosity value could be interpreted as ponded.

6. Conclusions and Future Research

The performance of the downscaling model at the Tarrawarra and Cache la Poudre catchments is reasonably good. The average NSCE values for the model at the Tarrawarra and Cache la Poudre catchments are 0.272 and 0.039, respectively. Those values are lower than the average NSCE values obtained by the EOF method, which is also a weighted combination of topographic patterns. However, this application of the model did not calibrate four of the model's parameters (due to the time required to implement such capabilities in the associated GIS tool). Thus, it is expected that the model's performance can be significantly improved. In addition, the model's basis in physical processes means that it can eventually make use of other information such as soil, vegetation, and climate data, which cannot be readily used in the EOF method. The EOF method also requires calculation of more topographic attributes, which increases the computational time required to downscale the patterns. Finally, the mathematical structure of the model means that it is less sensitive to scale effects than the EOF method.

Future research is needed along three lines. First, the model should be applied in a manner that fully exploits the available parameters. The vertical and horizontal pore-size distribution exponents can be calibrated separately as can the radiation and humidity-based exponents when the α parameter is allowed to take values other than zero. Second, more reliable parameter estimation methods should be explored. In the present application, the model was calibrated for two catchments with available soil moisture data and then applied to Afghanistan where soil moisture observations are not available. It is unlikely that the calibrations developed

at these catchments are optimal for Afghanistan. More soil moisture datasets should be collected and used for calibration to allow the use of more direct analogs to regions of interest. In addition, strategies to estimate the model parameters from limited soil moisture observations or other data should be explored. Third, the model should be generalized to accept other types of data that are available at fine resolutions and are strongly associated with soil moisture variations. In particular, vegetation attributes can be inferred from remote-sensing observations at a fine resolution and are expected to impact soil moisture patterns.

Acknowledgments. We gratefully acknowledge financial support from the Army Research Office Terrestrial Sciences Program and the Engineering Research and Development Center. We thank Andre Dozier for embedding the model into the GIS-tool described in Section 3. We also thank George Mason for supplying the intermediate resolution soil moisture data from Afghanistan and coordinating the application of this work for mobility assessments.

References

Abrams, M., Bailey, B., Tsu, H., and Hato, M., 2010, The ASTER Global DEM, Photogrammetric Engineering and Remote Sensing, 76(4), 344-348.

Ahmad, M.-u.-D., and Bastiaanssen, W.G.M., 2003, Retrieving soil moisture storage in the unsaturated zone using satellite imagery and bi-annual phreatic surface fluctuations, Irrigation and Drainage Systems, 17, 141-161.

AWFA, 2002, Data format handbook for AGRMET, Available online at http://www.rap.ucar.edu/projects/land/LSM/gribdoc/GRIB_HANDBOOK_FOR_LSMvariables.doc.

Beven, K.J. and Kirkby, M.J., 1979, A physically based variable contributing area model of basin hydrology, Hydrological Sciences, 24, 43-69.

Burt, T.P. and Butcher, D.P., 1985, Topographic controls of soil moisture distributions, Journal of Soil Science, 36, 469-486.

Busch, F.A., Niemann, J.D., and M.L. Coleman, 2011, Evaluation of the portability of an EOF-based method to downscale soil moisture patterns based on topographic attributes, MS Thesis, Colorado State University, Fort Collins, Colorado, 53 pp.

Campbell, G.S., 1974, A simple method for determining unsaturated conductivity from moisture retention data, Soil Science, 117(6), 311-314.

Chow, V.T., Maidment, D.R., and Mays, L.W., 1988, Applied Hydrology, McGraw Hill, New York, 572 pp.

Coleman, M.L., Dozier, A.Q., Fields, C.M., and Niemann, J.D., 2011, DownscaleConcept 2.3 User Manual: Downscaled, Spatially Distributed Soil Moisture Calculator, Army Research Office Technical Report.

Desilets, D., Zreda, M., and Ferré, T.P.A., 2010, Nature's neutron probe: Land surface hydrology at an elusive scale with cosmic rays, Water Resources Research, 46, W11505, doi:10.1029/2009WR008726.

Dingman, S. L., 2002, Physical Hydrology, 2nd edition, Prentice Hall, Upper Saddle River, New Jersey, 646 pp.

Entekhabi, D., Rodriguez-Iturbe, I. and Bras, R.L., 1991, Variability in large-scale water balance with land surface-atmosphere interaction, Journal of Climate, 5, 798-813.

Entekhabi, D., Njoku, E.G., Houser, P., Spencer, M., Doiron, T., Kim, Y., Smith, J., Girard, R., Belair, S., Crow, W., Jackson, T.J., Kerr, Y.H., Kimball, J.S., Koster, R., McDonald, K.C., O'Neill, P.E., Pultz, T., Running, S.W., Shi, J., Wood, E., and van Zyl, J., 2004, The hydrosphere state (Hydros) satellite mission: an Earth system pathfinder for global mapping of soil moisture and land freeze/thaw, IEEE Transactions on Geoscience and Remote Sensing, 42, 10, 2184-2195.

ESRI®, 2006, ArcMap™, Redlands, CA, Environmental Systems Research Institute, Inc.

Famiglietti, J.S., Dongryeol, R., Berg, A.A., Rodell, M., and Jackson, T.J., 2008, Field observations of soil moisture variability across scales, Water Resources Research, 44, W01423.

Fleming, K., Hendrickx, J.M.H., and Hong, S., 2005, Regional mapping of root zone soil moisture using optical satellite imagery, Proceedings of the SPIE, 5811, 159-170.

Grayson, R.B., Western, A.W., Chiew, F.H.S. and Bloschl, G., 1997, Preferred states in spatial soil moisture patterns: Local and nonlocal controls, Water Resources Research, 33(12), 2897-2908.

Kitanidis, P.K., and Bras, R.L., 1980, Real time forecasting with a conceptual hydrologic model. 2. Application and results, Water Resources Research, 16, 1034-1044.

Lehman, B. M. and J. D. Niemann, 2009, Controls on Spatial Patterns of Soil Moisture in a Semiarid Montane Catchment with Aspect-Dependent Vegetation, AGU Hydrology Days 2009, Fort Collins, CO.

Lin, H.S., Kogelmann, W., Walker, C. and Bruns, M.A., 2006, Soil moisture patterns in a forested catchment: A hydropedological perspective, Geoderma, 131, 345-368.

Mason, G.L., and Baylot, E.A., 2009, Procedures for predicting soil strength in terms of cone index for trafficability, unpublished manuscript.

Mason, G., Ahlvin, R., and Green, J., 2001, Short-Term Operational Forecasts of Trafficability, Geotechnical and Structures Laboratory, U.S. Army Corps of Engineers, Engineer Research and Development Center, ERDC/GSL TR-01-22.

Mathworks, 2009, Matlab®, Natick, MA.

Moore, I.D., Norton, T.W., and Williams, J.E., 1993, Modelling environmental heterogeneity in forested landscapes, Journal of Hydrology, 150, 717-747.

Noborio, K., 2001, Measurement of soil water content and electrical conductivity by time domain reflectometry: a review, Computers and Electronics in Agriculture, 31, 213-237.

Ntelekos, A.A., Georgakakos, K.P. and Krajweski, W.F., 2006, On the uncertainties of flash flood guidance: toward probabilistic forecasting of flash floods, Journal of Hydrometeorology, 7, 896-915.

Perry, M.A., and Niemann, J.D., 2007, Analysis and estimation of soil moisture at the catchment scale using EOFs, Journal of Hydrology, 334, 388-404.

Perry, M.A., and Niemann, J.D., 2008, Generation of soil moisture patterns at the catchment scale by EOF interpolation, Hydrology and Earth System Science, 12, 39-53.

Robinson, D.A., Jones, S.B., Wraith, J.M., Or, D., and Friedman, S.P., 2003, A review of advances in dielectric and electrical conductivity measurement in soils using time domain reflectometry, Vadose Zone Journal, 2, 444-475.

Rodriguez-Iturbe, I., Entekhabi, D. and Bras, R.L., 1991, Nonlinear dynamics of soil moisture at climate scales, Water Resources Research, 27(8), 1899-1906.

Scott, C.A., Bastiaanssen, W.G.M., and Ahmad, M-u-D, 2003, Mapping root zone soil moisture using remotely sensed optical imagery, Journal of Irrigation and Drainage Engineering, 129(5), 326-335.

Seyfried, M.S., 1998, Spatial variability constraints to modeling soil water at different scales, Geoderma, 85, 231-254.

Shuttleworth, W.J., Zreda, M., Zeng, X., Zweck, C., and T.P.A. Ferré, 2010, The COsmic-ray Soil Moisture Observing System (COSMOS): A non-invasive, intermediate scale soil moisture measurement network, BHS Third International Symposium, Managing Consequences of a Changing Global Environment, British Hydrological Society, Newcastle, 1-7.

Tarboton, D.G., 1997, A New Method for the Determination of Flow Directions and Contributing Areas in Grid Digital Elevation Models, Water Resources Research, 33(2), 309-319.

Western, A. W. and R. B. Grayson, 1998, The Tarrawarra data set: Soil moisture patterns, soil characteristics, and hydrological flux measurements, Water Resources Research 34(10), 2765-2768.

Western, A.W., Grayson, R.B., Blöschl, G., Willgoose, G.R. and McMahon, T.A., 1999, Observed spatial organization of soil moisture and its relation to terrain indices, Water Resources Research, 35(3), 797-810.

Wilson, D.J., Western, A.W. and Grayson, R.B., 2005. A terrain and data-based method for generating the spatial distribution of soil moisture. Advances in Water Resources 28, 43-54.